

DOI: 10.17725/rensit.2020.12.087

Mechanisms of dielectric relaxation of hexagonal ice

Airat A. Khamzin, Ivan V. Lunev

Kazan Federal University, <https://kpfu.ru/>

Kazan 420008, Russian Federation

E-mail: airat.khamzin1976@gmail.com, lunev75@mail.ru

Ivan I. Popov

Oak Ridge National Laboratory, <https://www.ornl.gov/>

Oak Ridge, Tennessee 37831, United States

E-mail: popovii@ornl.gov

Anna M. Greenbaum, Yuri D. Feldman

Hebrew University of Jerusalem, <https://new.huji.ac.il/en/>

Jerusalem 9190401, Israel

E-mail: Anechka@mail.huji.ac.il, yurif@mail.huji.ac.il

Received February 04, 2020; peer reviewed February 14, 2020; accepted February 18, 2020

Abstract. The article presents the results of theoretical and experimental studies of the dielectric relaxation of hexagonal ice in a wide temperature range. The model of dielectric relaxation of ice was developed explaining the origin of the dynamic crossovers in relaxation time at high and low temperatures. The results of the model are in agreement with experimental studies and explain the irreproducibility of dielectric experiments at low temperatures.

Keywords: hexagonal ice, dielectric relaxation, orientation defects, ionic defects, Cole-Cole relaxation

PACS: 77.22.Gm; 77.22.Ch; 66.10.Ed; 61.72.-y; 61.72.Bb

For citation: Airat A. Khamzin, Ivan I. Popov, Ivan V. Lunev, Anna M. Greenbaum, Yuri D. Feldman.

Mechanisms of dielectric relaxation of hexagonal ice. *RENSIT*, 2020, 12(1):87-94; DOI: 10.17725/rensit.2020.12.087.

CONTENTS

1. INTRODUCTION (87)

2. A MODEL OF THE TEMPERATURE CROSSOVERS OF RELAXATION TIME (88)

3. COMPARISON WITH THE EXPERIMENT (91)

4. CONCLUSION (92)

REFERENCES (93)

1. INTRODUCTION

Despite the intensive experimental and theoretical study of the electrical properties of hexagonal ice I_h [1-24], there is still no unified understanding of the physical mechanisms governing the observed relaxation behavior. Hexagonal ice is a relatively simple crystalline system with hydrogen bonds and its structure is well known [16–17], however, the dielectric relaxation behavior is rather complex (see Fig. 1).

The main peak of the dielectric losses of ice is symmetrically broadened below the temperature of 240 K and is well

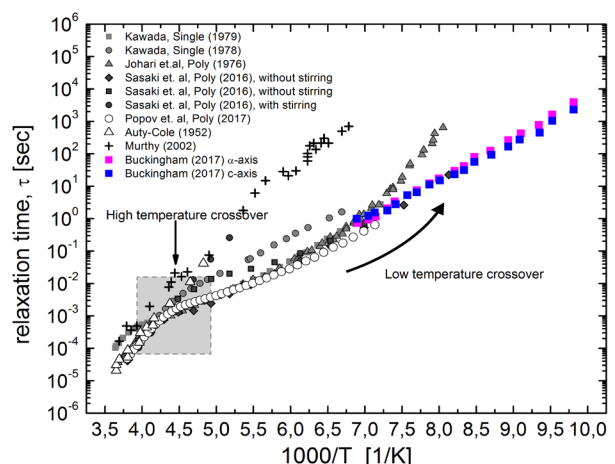


Fig. 1. The temperature dependences of the relaxation time of ice I_h . Gray squares and circles correspond to the data of single crystal [6, 7]; gray triangles correspond to polycrystals [4]. The data depicted in black circles, squares and rhombuses are taken from [9], white circles are the data from [25], white triangles from [1], black crosses from [8], pink and blue squares from [11].

described by the Cole-Cole expression for the complex dielectric permittivity (CDP) $\varepsilon^*(\omega) = \varepsilon_\infty + (\varepsilon_s - \varepsilon_\infty)/(1 + (i\omega\tau)^\alpha)$, where ε_∞ is the high-frequency limit of the dielectric permittivity, ε_s is the static dielectric permittivity, τ is the characteristic dielectric relaxation time, α is the peak broadening parameter of dielectric loss ($\alpha \leq 1$). Above temperature of 240 K, the main peak of the imaginary part of the CDP has a Debye shape ($\alpha = 1$). One of the most interesting experimental fact is related to the temperature behavior of the relaxation time τ (see Fig. 1). The Fig. 1 shows the temperature dependences of the dielectric relaxation time τ of ice I_h from different studies [1, 4, 6-9, 11, 25]. In early works [1] it was shown that above 200 K [2-7] the characteristic relaxation time of ice follows the Arrhenius law with an activation energy of 53.2 kJ/mol. However, the next later studies demonstrate a deviation from the Arrhenius behavior in the temperature range 210–245 K and a change in the slope of the relaxation time in logarithmic scale with a decrease in the activation energy down to 18.8 kJ/mol (see Fig. 1) [5-8]. It was demonstrated [9] that this transition or high-temperature crossover (HTC) depends on a method of ice samples preparation. Detailed measurements of the CDP of ice samples prepared by various methods [9] showed that samples prepared with stirring at water freezing (in order to avoid rapid ice crystallization) did not exhibit HTC, in contrast to the samples with regular freezing (without stirring). Detailed experiments performed in a wide temperature range [4, 5, 7] demonstrate also a second low-temperature crossover (LTC) below the temperature of ~ 170 K,

where activation energy rises up to 46.4 kJ/mol [5]. Furthermore, there is the discrepancy in the reproducibility of LTC.

In this paper, we discuss the main aspects of our understanding [12, 25-28] of the mechanisms that regulate the observed relaxation behavior of hexagonal ice (see Fig. 1) in a wide temperature range.

2. A MODEL OF THE TEMPERATURE CROSSOVERS OF RELAXATION TIME

Despite a very detailed experimental study of the dielectric properties of hexagonal ice, the theoretical study is lagging [12-17]. The Jaccard phenomenological theory [13-14] and the “*wait and switch*” model [16, 17, 22-24] are the most common nowadays. According to the latter, the presence of a network of hydrogen bonds in ice restricts the rotational diffusion of water dipoles and, therefore, the reorientation of dipole moments does not occur freely in ice. Crystalline ice is a well-ordered structure in terms of oxygen sites and, at the same time, it has certain disordering in terms of hydrogens position. Proton hopping create defects of two types in the ice structure: ionic and orientation (see Fig. 2). In the first case, the proton jumps along the hydrogen bond from one H_2O molecule to another [18] (see Fig. 2a) creating the ionic defects H_3O^+ and OH^- . While in the second, the proton moves to the neighboring hydrogen bond of the same H_2O molecule (see Fig. 2b), resulting in formation of a pair of Bjerrum L and D orientation defects [19-21]. Formally, such a jump can be considered as a rotation of H_2O molecule. These defects can diffuse over the ice crystal lattice. According to the “*wait and switch*” model [16, 17, 22-24], the

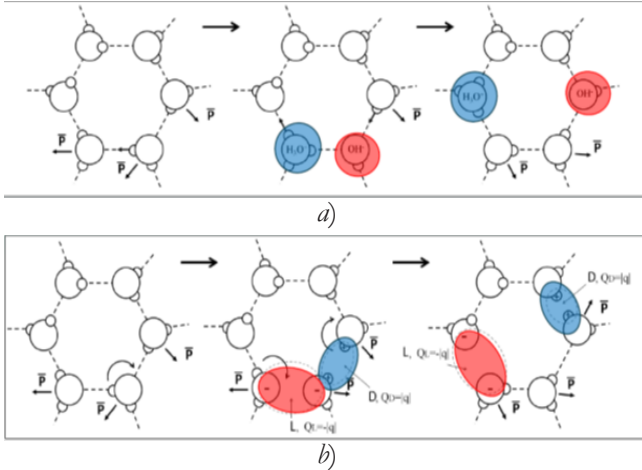


Fig. 2. Schematic presentation of the generation and the migration of pairs of ionic $\text{H}_3\text{O}^+/\text{OH}^-$ [12]- (a) and pairs of orientation L- and D-defects (b) in ice I_h with a change in the direction of the dipole moments of water molecules. Reproduced from ref. 12 with permission from the Royal Society of Chemistry.

reorientation of water molecule is the result of an intermittent change in the direction of its dipole moment. In this case, the reorientation of water molecule dipole is possible only when it encounters a corresponding defect in the hydrogen bonds network, otherwise the water molecule remains in a waiting mode (see Fig. 2).

The advantage of this approach is that it simplifies the theoretical analysis. Instead of investigating the problem of many bodies interaction, we can consider the problem of a random walk of defects. Based on this idea, the relationship between the CDP and the mean square displacement (MSD) of the defects $g(t) = \langle r^2(t) \rangle$ was derived [12]

$$\epsilon^*(\omega) = \epsilon_\infty + \frac{\epsilon_s - \epsilon_\infty}{1 + \left[\frac{1}{i\omega\epsilon_0} (\sigma_{LD}^*(\omega) + \sigma_\pm^*(\omega)) \right]^{-1}}, \quad (1)$$

$$\sigma_\alpha^*(\omega) = -\omega^2 \frac{n_\alpha q_\alpha^2}{6T} \hat{g}_\alpha(i\omega), \quad \alpha = LD, \pm.$$

where n_α , q_α , $\sigma_\alpha^*(\omega)$, $\hat{g}_\alpha(i\omega)$ are the density, the effective charge, the conductivity, and the Laplace image of the MSD of the defect

α , respectively, and T is the temperature in the energy units. It was shown in [12], that orientation defects obey normal diffusion law ($\langle r^2(t) \rangle = 6D_{LD}t$), while ionic defects demonstrates the anomalous diffusion behavior ($\langle r^2(t) \rangle = 6D_\pm t^{\alpha_\pm}$). Currently, there are large number of approaches, where anomalous diffusion motion might be derived. The most reasonable for the ice is based on the effect of ionic defects blockage created by orientation defects. For example, the H_3O^+ ionic defect jump can be blocked by orientation D-defects (see Fig. 3), then its further migration is impossible until at least one of D-defects moves away. Blocking of ionic defect jumps also occurs, when an H_3O^+ ion has passed through a certain fragment of the H-bonded network, and, as a result, the next ion would not be able to move along the same path. The release of the path is possible when a D-defect passes through it. Same is fair for the OH^- and L defects. Thus, the protons in ice structure may be trapped and localized for certain period of time that might lead to anomalous diffusion behavior. Taking it into account and based on the expression (1), the CDP of ice can be presented as follows [12]

$$\epsilon^*(i\omega) = \epsilon_\infty + \frac{\epsilon_s - \epsilon_\infty}{1 + \left[(i\omega\tau_{LD})^{-1} + (i\omega\tau_\pm)^{-\alpha_\pm} \right]^{-1}}. \quad (2)$$

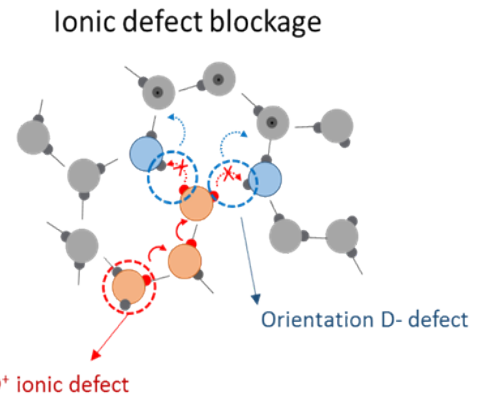


Fig. 3. Schematic presentation of possible blockage of proton hopping by Bjerrum orientation defects.

where

$$\tau_{LD} = \frac{T\varepsilon_0}{n_{LD}q_{LD}^2D_{LD}}, \quad \tau_{\pm}^{\alpha_{\pm}} = \frac{T\varepsilon_0}{\Gamma(1+\alpha_{\pm})n_{\pm}q_{\pm}^2D_{\pm}}. \quad (3)$$

determine the characteristic relaxation times of orientation L - D and ion defects, respectively.

The expression (2) for the CDP describes well the symmetrically broadened dielectric loss spectra for exponents α_{\pm} slightly deviating from the unity [12]. Moreover, assuming the Arrhenius behavior of the relaxation times $\tau_{LD,\pm} = \tau_{LD,\pm}^{\infty} \exp(E_{LD,\pm}/T)$, the temperature dependence of the relaxation time τ , determined by the position of the maximum of the imaginary part of the CDP (2), well describes the HTC [12, 28]. Here $E_{LD,\pm}$ are the activation energies of the orientation and ionic defects, respectively. Due to the large difference in the activation energies of orientation and ionic defects ($E_{LD} > E_{\pm}$), the relaxation time through the orientation defects is much smaller in compare to that of ionic defects at high temperatures, $\tau_{LD} \ll \tau_{\pm}$, leading to that the overall relaxation mechanism goes through the orientation defects diffusion and $\tau \approx \tau_{LD}$. With temperature decrease the orientation defects motion slows down and at temperatures below 240 K one have $\tau_{LD} \gg \tau_{\pm}$, i.e. the relaxation mechanism of ion defects starts to play a dominant role and $\tau \approx \tau_{\pm}$. Thus, on a logarithmic scale, the temperature dependence of the relaxation time changes the slope with decreasing the activation energy from E_{LD} to $E_{\pm} < E_{LD}$. The temperature of HTC temperature, T_{c1} is determined then by $\tau_{LD}(T_{c1}) = \tau_{\pm}(T_{c1})$ and is equal to

$$T_{c1} = \frac{E_{LD} - E_{\pm}}{\ln(\tau_{\pm}^{\infty} / \tau_{LD}^{\infty})}. \quad (4)$$

Thus, an alteration in the activation energy at the temperatures about 240 K is due to the transition from the dominant motion of orientation defects at high temperatures to the dominant motion of ionic defects at low temperatures.

At lower temperatures (below 170 K), the motion of orientation defects significantly slows down, forming sufficiently “deep” traps for ionic defects. As a result, it causes the creation of ion-orientation complexes [25, 28]. These structures determine the further relaxation of ice by creating a new type of complex protons diffusion motion correlated with the movements of the orientation defects. Thus, the following expression for the CDP of hexagonal ice can be obtained [25, 28]

$$\varepsilon^*(i\omega) = \varepsilon_{\infty} + \frac{\varepsilon_s - \varepsilon_{\infty}}{1 + \left[(i\omega\tau_{LD})^{-1} + \left((i\omega\tau_{\pm})^{\alpha_{\pm}} + (i\omega\tau_t)^{\alpha_t} \right)^{-1} \right]^{-1}}, \quad (5)$$

where τ_{\pm} is determined by the expression (3), $\tau_t^{\alpha_t} = T\varepsilon_0 / \Gamma(1+\alpha_t)n_{\pm}q_{\pm}^2D_t$, where D_t , α_t are the effective diffusion coefficient and the anomalous diffusion coefficient of protons in traps, correspondingly. In case of exponents α_{\pm} and α_t are close to one, the expression (5) can be reduced to the Cole–Cole law [25, 28]. The temperature of the second, low-temperature “crossover” T_{c2} (LTC temperature), is determined from $\tau_{\pm}(T_{c2}) = \tau_t(T_{c2})$, where $\tau_t = \tau_t^{\infty} \exp(E_t/T)$, and is equal to

$$T_{c2} = \frac{E_t - E_{\pm}}{\ln(\tau_{\pm}^{\infty} / \tau_t^{\infty})}. \quad (6)$$

3. COMPARISON WITH THE EXPERIMENT

To demonstrate the qualitative and quantitative agreement of theoretical model to experimental data, we performed the numerical fitting procedure for the relaxation times [4, 7, 25] and peak broadening parameter [25] by the theoretical dependences derived from the model [25,28]. The results are presented in the **Table 1** and in the **Fig. 4**. One can see that the proposed theoretical expressions are in a good agreement with the corresponding experimentally observed behavior (see Fig. 4). It indicates the consistency of the proposed model of the dielectric relaxation of ice I_h . Note, that the estimated activation energies of orientation L - D defects and ion defects for the experiments of [4, 7, 25] are in good agreement between each other (see Table 1). However, the E_i of the data of [7, 25] significantly differs from the estimates for the data taken from [4].

The experimental results of the dielectric response of hexagonal ice for various temperature protocols is presented in [25]. As it has been noted in the introduction, there is an irreparability of dielectric results at low temperatures. Most likely, this is because the microstructure (polycrystallinity) of ice depends on the temperature protocol, leading to variability of the correlation between the ionic and orientation defects. Indeed, a series of studies [29–31] using

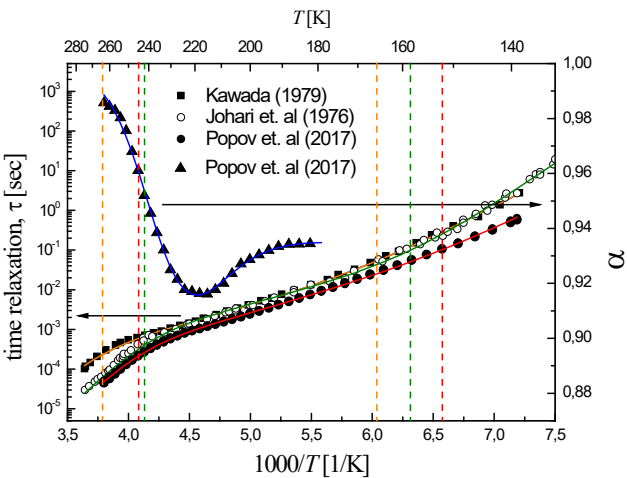


Fig. 4. A graphical presentation of the results of numerical fitting of the experimental data from [4] (white circles), [7] (black squares), [25] (black circles) for the relaxation time $\tau(T)$ and the broadening parameter of the dielectric loss peak $\alpha(T)$ [25] (black triangles) using theoretical dependences for τ (solid green, orange, and red lines for the data of [4], [7], [25], respectively) and α (solid blue line) from [25, 28]. The vertical dashed lines indicate the position of the “crossovers” temperatures (the color of the lines corresponds to the colors of the fitting curves for the relaxation time of [4], [7], [25], correspondingly). Reproduced from ref. 28 with permission of the copyright owner.

X-ray diffraction topography revealed interstitial defects in the ice crystals structure, whose concentration increases rapidly during cooling. However, any micro dislocations and cracks in ice, can be a source of L - D defects and might be considered as additional suppressors of proton migration over long distances.

The experimental results obtained in [25] confirm the above assumption that the dielectric response of ice I_h strongly depends on its preparation and the temperature protocol. Furthermore, we observe a

Table1

The model parameters obtained from the numerical fitting of the experimental data from [4], [7], [25] for the relaxation time and the broadening parameter of the dielectric loss peak [25] using theoretical dependences from [25, 28]. The values of α_{\pm} , α_i are related to each other by $\alpha_{\pm} \approx (\alpha_{\pm} + 1)/2$, and $\alpha_{\pm} \approx 0.92$ for all experiments. Reproduced from ref. 28 with permission of the copyright owner.

	E_{LD} , kJ/mol	$\tau_{LD}^{\infty} \cdot 10^{-16}$ s	E_{LD} , kJ/mol	$\tau_{\pm}^{\infty} \cdot 10^{-7}$ s	E_{LD} , kJ/mol	$\tau_i^{\infty} \cdot 10^{-13}$ s	T_{c1} , K	T_{c2} , K
Johari et al. [4]	56.92	4.06	15.25	4.52	40.54	0.0195	242	158.4
Kawada [7]	57.11	2.245	14.98	4.89	32.3	16.67	264	165.6
Popov et al.. [25]	57.6	2.25	15.74	1.97	31.27	8.88	244.9	152.1

difference in the dielectric response of ice even being prepared by the same procedure. We assume that this phenomenon is due to the uniqueness of the microstructure of the polycrystalline sample. Based on the proposed model, we imply that various microstructures of ice affect the migration of L - D and ionic defects, and, in particular, the correlation between different ice defects. The latter determines the dynamics at low temperatures, where the strongest discrepancy in the experimental results is observed. At high temperatures, the mobility of the defects is high and therefore any deviations in ice formation are averaged. Thus, all the measurements have approximately the same values of the dynamic parameters (α , τ) above the HTC ($T \approx 240$ K). Based on this assumption, we can explain the result obtained in [9], where the absence of HTC was detected in the ice sample prepared using the stirring procedure (see Fig. 1). Most probably, the stirring procedure causes tensions inside the ice lattice, which, in turn, leads to the formation of micro cracks during cooling. A large number of cracks can prevent proton migration and disable the relaxation mechanism caused by ion defects. In our model, this corresponds to a strong correlation between L - D and ionic defects when orientation-ionic aggregates appear.

4. CONCLUSION

In this paper, the results of the theoretical and the experimental studies of the dielectric relaxation of hexagonal ice [12, 25–28] are presented. We propose the mechanisms underlying in the relaxation behavior of the most common type of ice I_h in a wide temperature range. A simple phenomenological model of dielectric

relaxation of ice has been developed. It is based on the “wait and switch” model, where the migration of orientation and ionic defects along the ice lattice is considered as the main mechanism of dielectric relaxation. The concentration of orientation defects in ice is significantly greater than the concentration of ionic defects, and their activation energy is higher. Therefore, at high temperatures (above 240 K), the relaxation occurs mainly due to the migration of orientation defects. However, when the temperature decreases, the relaxation mechanism through the orientation defects slows down due to their high activation energy, and the mechanism by ionic defects starts to dominate. It causes the high-temperature crossover near 240 K. Because of the orientation defects are essentially the breaks in hydrogen bonds structure of ice, they can block the proton jumps by creating of so-called proton “traps”, and, therefore, restrict the migration of ionic defects. As a result, the diffusion of ionic defects slows down and becomes abnormal. This abnormal diffusion of ionic defects is the reason for the broadening of the dielectric loss peak in ice. With a further decrease in temperature, the processes of proton trapping begins to dominate. Thus, the number of delocalized protons increases and the relaxation process slows down again. Therefore, a smooth increase in the relaxation time behavior is observed at low temperatures (low-temperature crossover).

Based on the detailed dielectric measurements presented in [25], the one of the main reason for the irreproducibility of the experimental data at low temperature region was ascribed to the effect of sample preparation procedure on the ice microstructure and used temperature

protocol. The formed ice microstructure significantly affects the migration of orientation and ionic defects, in particular, their correlated diffusion. The presence of impurities and various defects, such as dislocations and micro cracks, leads to the increase of the number of the orientation defects. It, in turn, leads to a complete or partial blocking of the relaxation mechanism via the proton hopping, resulting the temperature dependence of the relaxation time corresponding to the migration of ionic defects.

REFERENCES

1. Auty PP and Cole RH. Dielectric properties of ice and solid D_2O . *J. Chem. Phys.*, 1952, 20:1309-1314.
2. Johari GP, Jones SJ. The orientation polarization in hexagonal ice parallel and perpendicular to the c-axis. *J. Glaciol.*, 1978, 21:259-276.
3. Gough SR, Davidson DW. Dielectric behavior of cubic and hexagonal ices at low temperatures. *J. Chem. Phys.*, 1970, 52:5442.
4. Johari GP, Jones SJ. Dielectric properties of polycrystalline D_2O ice I_h (hexagonal). *Proc. R. Soc. A*, 1976, 349:467-495.
5. Johari GP, Whalley E. The dielectric-properties of ice I_h in the range 272-133 K. *J. Chem. Phys.*, 1981, 75:1333-1340.
6. Kawada S. Dielectric anisotropy in ice I_h . *J. Phys. Soc. Jpn.*, 1978, 44:1881-1886.
7. Kawada S. Dielectric-properties of heavy ice I_h (D_2O ice). *J. Phys. Soc. Jpn.*, 1979, 47:1850-1856.
8. Murthy SSN. Slow relaxation in ice and ice clathrates and its connection to the low-temperature phase transition induced by dopants. *Phase Transitions*, 2002, 75:487-506.
9. Sasaki K, Kita R, Shinyashiki N, Yagihara S. Dielectric relaxation time of ice- I_h with different preparation. *J. Phys. Chem. B*, 2016, 120:3950-3953.
10. Worz O, Cole RH. Dielectric properties of ice I_h . *J. Chem. Phys.*, 1969, 51:1546.
11. Buckingham DTW. High-resolution thermal expansion and dielectric relaxation measurements of H_2O and D_2O ice I_h . *PhD Thesis*, Montana State University, 2017.
12. Popov I, Puzenko A, Khamzin A, Feldman Y. The dynamic crossover in dielectric relaxation behavior of ice I_h . *Phys. Chem. Chem. Phys.*, 2015, 17:1489-1497.
13. Jaccard C. *Etude Th'éorique et Exp'érimentale des Propri'et'es 'electriques de la Glace*. Institut de Physique, E.P.F., Zürich, 1959.
14. Jaccard C. Thermodynamics of irreversible processes applied to ice. *Phys. Condens. Mater.*, 1964, 3:99-118.
15. Eisenberg DS, Kauzmann W. *The Structure and Properties of Water*. Clarendon Press, Oxford University Press, Oxford, New York, 2005.
16. Hobbs PV. *Ice Physics*. Oxford University Press, New York, 2010.
17. Petrenko VF, Whitworth RW. *Physics of Ice*. Oxford University Press, Oxford, New York, 1999.
18. Agmon N. The Grotthuss mechanism. *Chem. Phys. Lett.*, 1995, 244:456-462.
19. Bjerrum N. Structure and properties of ice. *Science*, 1952, 115:385-390.

20. Grishina N, Buch V. Structure and dynamics of orientational defects in ice I. *J. Chem. Phys.*, 2004, 120:5217-5225.
21. Podeszwa R, Buch V. Structure and dynamics of orientational defects in ice. *Phys. Rev. Lett.*, 1999, 83:4570-4573.
22. Sciortino F, Geiger A, Stanley HE. Effect of defects on molecular mobility in liquid water. *Nature*, 1991, 354:218-221.
23. Sciortino F, Geiger A, Stanley HE. Network defects and molecular mobility in liquid water. *J. Chem. Phys.*, 1992, 96:3857-3865.
24. Vonhippel A. The dielectric-relaxation spectra of water, ice, and aqueous solutions, and their Interpretation. 3. Proton organization and proton-transfer in ice. *IEEE Trans. Electr. Insul.*, 1988, 23:825-840.
25. Popov I, Lunev I, Khamzin A, Greenbaum A, Gusev Y, Feldman Y. The low-temperature dynamic crossover in dielectric relaxation of ice I_h . *Phys. Chem. Chem. Phys.*, 2017, 19:28610.
26. Khamzin AA, Nigmatullin RR. Multiple-trapping model of dielectric relaxation of the ice I_h . *J. Chem. Phys.*, 2017, 147(20):204502.
27. Khamzin AA, Nasybullin AI. Trap-controlled proton hopping: interpretation of low-temperature dielectric relaxation of ice I_h . *Phys. Chem. Chem. Phys.*, 2018, 20(35):23142-23150.
28. Khamzin AA, Nasybullin AI. Langevin approach to the theory of dielectric relaxation of ice I_h . *Physica A*, 2018, 508:471-480.
29. Goto K, Hondoh T, Higashi A. Determination of Diffusion Coefficients of Self-Interstitials in Ice with a New Method of Observing Climb of Dislocations by X-Ray Topography. *Jpn. J. Appl. Phys.*, 1986, Part 1, 25:351-357.
30. Hondoh T, Itoh T, Amakai S, Goto K, Higashi A. Formation and annihilation of stacking faults in pure ice. *J. Phys. Chem.*, 1983, 87:4040-4044.
31. Hondoh T, Itoh T, Higashi A. Formation of Stacking Faults in Pure Ice Single Crystals by Cooling. *Jpn. J. Appl. Phys.*, 1981, 20:L737-L740.